Latin American Journal of Pharmacy
(formerly *Acta Farmacéutica Bonaerense)*
Lat. Am. J. Pharm. **30** (1): 126-31 (2011)

Original Article
Received: April 16, 2010
Revised version: May 11, 2010
Accepted: May 12, 2010

Physicochemical Characterization of $La_2(CO_3)_3.4H_3O$, a New and Promising Agent for the Treatment of Hyperphosphatemia

Enrique J. BARAN *

Centro de Química Inorgánica (CEQUINOR, CONICET/UNLP), Facultad de Ciencias Exactas, Universidad Nacional de La Plata, C. Correo 962, 1900-La Plata, Argentina.

***SUMMARY*. The synthesis of $La_2(CO_3)_3.4H_2O$ was carefully investigated, on the basis of the thermal behavior (TG and DTA measurements) of the corresponding octahydrate, used as the precursor. The analysis of the X-ray powder diagrams of $La_2(CO_3)_3.4H_2O$ showed that this hydrate crystallizes in the tetragonal crystal system with Z = 8. The FTIR and FT-Raman spectra of $La_2(CO_3)_3.4H_2O$ and of $La_2(CO_3)_3.8H_2O$ were recorded and assigned. The usefulness of the tetrahydrate for the treatment of hyperphosphatemia is briefly discussed.**

INTRODUCTION

Renewed interest on the pharmacological properties of lanthanide compounds has lately increased [1-6]. Although the use of different complexes of this group of elements, particularly Gd(III), as NMR contrast imaging agents is well known and established [4,6-8], other concrete medical applications begin only slowly to emerge and, among them, the use of lanthanide complexes for the treatment of bone disorders [5] and hyperphosphatemia [4,6] are particularly interesting and relevant.

Phosphorus is the sixth most abundant element in the human body [9]. It exists in many inorganic and organic forms and is of central importance for energy metabolism, bone mineralization, cellular structure and genetic coding [10]. Up to 80-90% of the element is found in bone. Phosphorous homeostasis is normally maintained through several mechanisms. Gastrointestinal absorption must be matched by renal excretion, and cellular release is balanced by uptake in other tissues. Hyperphosphatemia, increased serum phosphate levels, occurs when the phosphorous load (from gastrointestinal absorption, exogenous administration, or cellular release) exceeds renal excretion and tissue uptake. It is usually one of the clinical consequences that accompanies end stage renal disease (ESRD) [4,6].

Phosphate metabolism is intimately related to calcium metabolism and is regulated by parathyroid hormone and vitamin D. The hormone controls phosphate balance in the body by lowering tubular reabsorption of phosphate by the kidney. Consequently, during renal impairment hormone secretion increases in an attempt to further decrease phosphate reabsorption, and correct the hyperphosphatemia. Furthermore, vitamin D metabolism in the kidney is impaired in ESRD resulting in reduced calcium absorption and hypocalcemia. This decrease in calcium can, in turn, stimulate parathyroid hormone secretion. In this way, the organism attempts to correct for the high phosphate levels, but at the expense of increased parathyroid activity, a state described as secondary hyperparathyroidism [4,6,11]. In addition, hyperphosphatemia and hypo-

KEY WORDS: Crystallographic data, Hyperphosphatemia, Lanthanum carbonate tetrahydrate, Thermal behavior, Vibrational spectra.

* Author to whom correspondence should be addressed. *E-mail:* baran@quimica.unlp.edu.ar

ISSN 0326-2383

calcemia are associated with atherosclerosis, uremic bone disease and soft-tissue calcification [4,11].

Although hypocalcemia and secondary hyperparathyroidism can be treated with calcium supplements and the vitamin D derivative calcitriol, hyperphosphatemia can interfere with these therapies. This means that alternative options are needed and usually phosphate binders are employed [4,6,11,12]. Aluminum salts, such as the hydroxide, which are effective phosphate binders, have been initially used but have been abandoned because of its toxicity [4,6,12]. As a result, calcium phosphate binders gradually replaced aluminum-based phosphate binders, with calcium carbonate and acetate the most commonly used [6,12,13]. However, the problem with calcium-based agents is that the calcium can be absorbed resulting in hypercalcemia and increased risk of cardiovascular calcification, a situation that can be furtherly complicated if calcitriol is simultaneously used.

The commented concerns and challenges with aluminum- and calcium-based phosphate binders have stimulated research on the development of new aluminum- and calcium-free binders [4,6,14]. These studies finally lead to the development of a novel and very interesting agent, traded as *Fosrenol*®, based on lanthanum carbonate, and which use has been approved in 2004 by the FDA of the United States of America. It has also received approval in different European countries and in Japan. Very favorable pre-clinical pharmacokinetic and toxicological profiles for this drug have been reproduced in several Phase I and Phase II clinical studies [4]. Phase III clinical studies have been reported in both the United States and Europe [4,14]. These studies have shown that Fosrenol® is very effective in reducing high phosphate levels associated with ESRD, reduced the risk of hypercalcemia and showed long-term efficacy.

The best results were obtained with the tetrahydrate, $La_2(CO_3)_3.4H_2O$, with optimal phosphate-binding at pH 3-5, whilst retaining binding activity across the full pH range 1-7. This means that lanthanum carbonate can bind phosphate at the low pH of the stomach, as well as at the higher pH values found in the small intestine, duodenum and jejunum. It dissociates in the gastrointestinal tract to allow the formation of lanthanum phosphate and this insoluble phosphate is eliminated by the fecal route without significant absorption or tissue accumulation of La(III) [4].

In order to advance in a better characterization of this new and interesting phosphate-binder we have now investigated its crystallographic characteristics and vibrational-spectroscopic behavior. Besides, we have also performed the spectroscopic study of the chemical precursor of *Fosrenol*®, $La_2(CO_3)_3.8H_2O$, and analyzed its thermal degradation to generate $La_2(CO_3)_3.4H_2O$.

MATERIALS AND METHODS

The starting compounds for the syntheses were $LaCl_3.xH_2O$ (Merck) and $NaHCO_3$ (Carlo Erba). The precursor, $La_2(CO_3)_3.8H_2O$, can be obtained by different procedures: a) by direct precipitation, reacting La(III) and CO_3^{2-} aqueous solutions; b) by slow hydrolysis of urea in an aqueous solution containing the lanthanum salt [15]; c) by hydrolysis of lanthanum trichloroacetate [16]. We have used the first procedure, briefly described as follows: to 40 mL of a 0.1 M solution of $LaCl_3$, heated at 60 °C, 20 mL of a 0.6 M solution of $NaHCO_3$ was dropwise added, under constant stirring. The temperature and stirring were then maintained for five hours. After cooling, the precipitated white product was filtered off using a G3 glass fritted funnel and immediately washed with several portions of hot water. Finally, the precipitate was dried in air for several days. Its purity was checked by determination of the lanthanum content (weighing out the generated La_2O_3 after ignition at 800 °C) and by its characteristic X-ray powder diffractogram [15].

Based on the information provided by the study of the thermal decomposition of $La_3(CO_3)_3.8H_2O$ (see below) samples of the tetrahydrate were obtained by carefully controlled isothermal dehydration of the precursor at 80 °C. For precursor samples of about 200 mg, the reaction time was of approximately 120-150 min. Analytical data: % of La_2O_3 for four different preparations ranged between 61.45 and 61.53 % (Value calculated for $La_2(CO_3)_3.4H_2O$: 61.50 %).

Infrared spectra were recorded with a Bruker IFS 66 FTIR instrument, using the KBr pellet technique. Raman spectra were obtained with the FRA 106 accessory of the same spectrophotometer, using the 1064 nm radiation from a Nd : YAG laser for excitation. Thermogravimetric (TG) and differential thermal analysis (DTA) were performed on a Shimadzu system (models TG-50 and DTA-50, respectively), using platinum crucibles, working in an oxygen flow of

50 mL/min and at a heating rate of 5 °C/min. Sample quantities ranged between 10 and 20 mg. Al_2O_3 was used as a DTA standard. Powder diagrams were obtained with a Philips PW 1710 diffractometer, using Ni-filtered Cu-K_α radiation (λ = 1.5425 Å). The density of the $La_2(CO_3)_3.4H_2O$ samples was determined pycnometrically, at 25 °C, using benzene as the working liquid.

RESULTS AND DISCUSSION

Crystal structure of $La_2(CO_3)_3.8H_2O$

Crystallographic information on hydrated and anhydrous lanthanide carbonates remains relatively scarce [17]. Notwithstanding, the crystal structures of $La_2(CO_3)_3.8H_2O$ [18] and of the structurally related mineral lanthanite, $(Ce,La)_2(CO_3)_3.8H_2O$ [19], were solved some years ago. $La_2(CO_3)_3.8H_2O$ belongs to the orthorhombic space group Pccn (D_{2h}^{10}, Nr. 56) with Z = 4. The structure consists of two distinctive 10-coordinated La(III) polyhedra presenting a strongly distorted Archimedean antiprismatic geometry. One of these La(III) cations is coordinated by four water molecules and two unidentate and two bidentate carbonate groups and these four carbonate groups also act as bridges to the second cation. Around this second cation one bidentate carbonate anion replaces two water molecules. The structure consists of infinite layers of La-O coordination polyhedra and CO_3^{2-} groups. The facile micaceous cleavage observed along (001) supports this conjecture [18]. Besides, two of the water molecules are not bonded to the metal centers and are situated between the layers, participating in the hydrogen bonding arrangement which is involved in the stabilization of the structure.

For the subsequent spectroscopic discussion, it is important to remark that four of the CO_3^{2-}groups present in the unit cell are located on C_2 sites, whereas the remaining eight occupies general C_1 positions [18].

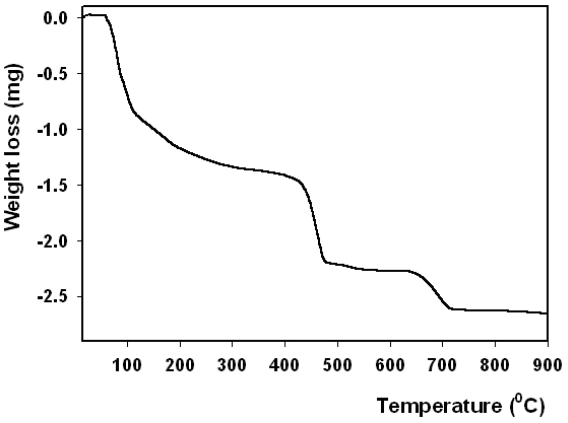

Figure 1. TG-trace of the thermal decomposition of $La_2(CO_3)_3.8H_2O$.

Thermal behavior of $La_2(CO_3)_2.8H_2O$

With the purpose of determining the best conditions for the partial dehydration of the carbonate precursor, we have investigated its thermal behavior by TG/DTA measurements. A typical thermogravimetric trace is shown in Figure 1 and as it can be seen, the decomposition occurs in three well-defined steps. A detailed analysis of the TG and DTG (first derivative of the mass change) curves is presented in Table 1.

In the first step, which extends between 25 and 232 °C, the greatest part of the water molecules was lost. A thorough analysis of the corresponding DTG traces shows that this process is related to three successive events, corresponding respectively to the elimination of 3.5, 2.3 and 1.65 moles of H_2O. Each of this events is accompanied by an endothermic DTA-signal, the third of which (175 °C) is very weak. In the subsequent step the rest of water, together with two CO_2 molecules is eliminated, with generation of lanthanum dioxocarbonate, according to:

$$La_2(CO_3)_3.0.55H_2O \rightarrow La_2O_2CO_3 + 2\ CO_2 + 0.55\ H_2O$$

This process is also accompanied by an endothermic DTA-signal, at 472 °C.

Lanthanide dioxocarbonates are recognized as stable intermediates in the thermal decomposition of the corresponding carbonates [20-22] and, in the present case, this intermediate decompos-

T-range (°C)	Δm-found	Product lost	Δm-calculated	DTA-signal
28 - 96	- 10.43%	- 3.5 H_2O	- 10.47%	82 °C, endo
96 - 138	- 6.88%	- 2.3 H_2O	- 6.87%	98 °C, endo
138 - 232	- 4.95%	- 1.65 H_2O	- 4.94%	175 °C, endo
232 - 575	- 16.56%	-0.55 H2O - 2 CO_2	- 16.28%	472 °C, endo
575 - 815	- 7.15%	- CO_2	- 7.31%	680 °C, endo

Table 1. Analysis of the thermogravimetric data for the decomposition of $La_2(CO_3)_3.8H_2O$.

es to the respective oxide in the last thermolysis step:

$$La_2O_2CO_3 \rightarrow La_2O_3 + CO_2$$

The transformation is complete at about 800 °C and is accompanied by an endothermic DTA signal at about 680 °C. In some of the recorded thermograms this signal shows a weak splitting into two components.

The final analysis of the data presented in Table 1, shows that the total expected weight loss for the transformation of $La_2(CO_3)_3.8H_2O$ into La_2O_3 is of 45.87 %, in excellent agreement with experimentally observed figure of 45.97 %.

The thermal behavior of the $La_2(CO_3)_3.8H_2O$ precursor, suggests that for the preparation of the desired tetrahydrate, careful thermal treatment in the temperature range between 80-85 °C is the obvious election. Therefore, in our synthesis procedures we have always worked at 80 °C, with optimal results.

X-ray powder diffractometry

As mentioned above, the X-ray powder diagram of $La_2(CO_3)_3.8H_2O$ is well-known [15] and was used for the characterization of this precursor. In spite of the fact that the X-ray powder diagram of $La_2(CO_3)_3.4H_2O$ looks simpler than that of the precursor, its general aspect suggests a poorer crystallinity of this material in comparison to that of the precursor. Attempting a wider characterization of the structural properties of the tetrahydrate, the recorded X-ray powder diagram was analyzed with the aid of a locally modified version of the Program PIRUM of Werner [23]. The results of this analysis are presented in Table 2 and show that this hydrate crystallizes in the tetragonal crystal system with eight formulas in the crystallographic unit cell.

Crystallographic data

Crystal system:	tetragonal	
Unit cell parameters (Å):	a = 17.49(2)	c = 9.60(1)
Volume (Å^3):	2936.64	
Density (g/mL)	Exp.: 2.4	Calc.: 2.39
Z	8	

Indexed X-ray powder diagram

h k l	$d_{observed}$	$d_{calculated}$	I/Io
2 2 0	6.211	6.187	100
2 2 1	5.144	5.201	3
0 0 2	4.812	4.802	95
1 1 2	4.496	4.477	37
2 2 2	3.812	3.794	15
5 1 0	3.441	3.432	12
5 0 1	3.285	3.288	65
0 0 3	3.199	3.201	20
4 2 2	3.032	3.033	9
6 0 0	2.912	2.916	24
5 3 1	2.867	2.864	20
5 2 2	2.692	2.691	5
7 2 0	2.405	2.404	4
2 0 4	2.315	2.315	6

Table 2. Crystallographic data and indexed powder diagram of $La_2(CO_3)_3.4H_2O$.

Vibrational spectroscopy

Partial information on the IR spectra of lanthanide carbonates are found in the literature [24-26] but attempts to correlate the spectroscopic behavior with the structural peculiarities and also information on the corresponding Raman spectra were not found. Besides, and as far as we know, spectroscopic investigations of partially dehydrated carbonates have also not been undertaken. Consequently, we have now performed a detailed IR and Raman spectroscopic study of $La_2(CO_2)_3.8H_2O$ and of the corresponding tetrahydrate. Figure 2 shows the IR spectra of both hydrates and the proposed assignment is presented in Table 3 and briefly commented below.

The "free" planar CO_3^{2-} anion (D_{3h}-symmetry) presents in solution four internal vibrational modes, *i.e.*, ν_1 (A_1', symmetric stretching = 1063 cm^{-1}), ν_2 (A_2", out of plane deformation = 880 cm^{-1}), ν_3 (E', antisymmetric stretching = 1415 cm^{-1}), ν_4 (E', antisymmetric bending = 680 cm^{-1}). The two E' modes are both IR and Raman

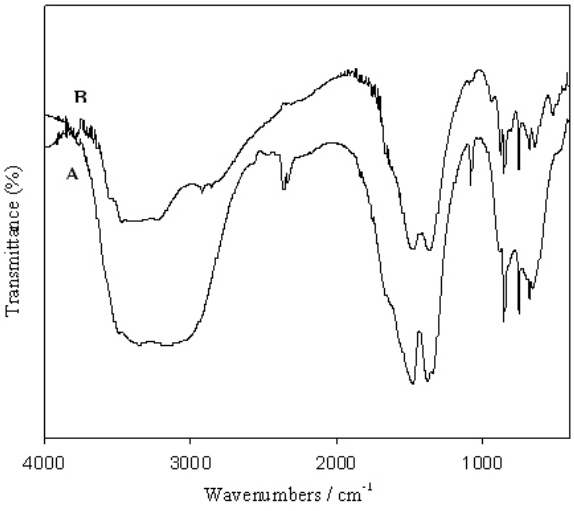

Figure 2. FTIR spectra of $La_2(CO_3)_3.8H_2O$ (**A**) and $La_2(CO_3)_3.4H_2O$ (**B**).

$La_2(CO_3)_3$ $8H_2O$		$La_2(CO_3)_3$ $4H_2O$		Assignment
IR	**Raman**	**IR**	**Raman**	
3505 w		3473 w		
3360 vs, br		3378 vs, br		ν(OH) (H_2O)
3170 vs, br		3235 w		
		2922w/2852w		Overtone
2467 vw				Combination
1667 sh		1640 sh		
1568 sh		1563 sh		
1475 vs		1477 vs		$\nu_{as}(CO_3)$, ν_3
1374 vs	1384 w	1365 vs		
1340 sh				
1076 m	1087vs/1068sh	1083 vw	1089vs/1064m	$\nu_s(CO_3)$, ν_1
		935 w		
881 vw	886 vw	873 m		
850 m		850 m		$\gamma(CO_3)$, ν_2
820 sh		820 sh		
746 m	759 m	747 m	764 m	$\delta_{as}(CO_3)$, ν_4
679 w		676 m		
648 vw		639 m		
480 sh		517 m		ν(La-O)(?)

Table 3. Assignment of the vibrational spectra of the two investigated hydrates of lanthanum(III) carbonate; **vs**: very strong; **m**: medium; **w**: weak; **vw**: very weak; **sh**: shoulder; **br**: broad.

active, whereas the A_1' mode is only Raman active and the A_2" mode only IR active [27].

After coordination, the symmetry of the carbonato ligand, in both monodentate or bidentate coordination, becomes C_{2v} [27,28] and, thus, all vibrations become IR and Raman active and the doubly degenerate vibrations, ν_3 and ν_4, splits into two bands and this splitting is usually larger in the case of bidentate carbonato groups [28]. Besides, the same spectral behavior is expected considering only the above mentioned site-symmetry conditions of the carbonate groups (four at C_2 sites and eight at C_1 sites).

The IR spectra of the tetrahydrate and of its precursor, shown in Figure 2, are relatively similar and only small changes in the intensity and form of some of the bands can be noted.

The Raman spectra are extremely simple and are dominated by the very strong ν_1-band, corresponding to the symmetric stretching of the carbonato groups. Interestingly, this strong band appears splitted and this splitting is more evident in the case of the tetrahydrate. The antisymmetric carbonato stretching, ν_3, is only observed as a weak Raman signal in the case of $La_2(CO_3)_3.8H_2O$ and is absent in the lower hydrate. The antisymmetric bending, ν_4, is found as a unique, medium intensity Raman band, in both cases.

The antisymmetric stretching, ν_3, clearly dominates both IR spectra. The widening of this band and the appearance of a fine structure is surely related to the presence of the structurally different carbonato groups in the crystal lattice. The corresponding symmetric stretching, ν_1, is only seen as a very weak IR signal for the tetrahydrate and is better defined in the case of the precursor.

The broad band related to the stretching modes of the H_2O molecules also originates in the great number of molecules present in these materials and the different characteristics of its interactions in the lattice. Interestingly, this band appears somewhat better defined and less widened in the case of $La_2(CO_3)_3.4H_2O$, in agreement with the existence of a more reduced number of water molecules in this material. The deformational modes of these molecules, expected to lie at around 1600-1650 cm^{-1}, surely contribute appreciably to the commented widening of $\nu_3(CO_3)$ band.

The ν_2 and ν_4 components, although lying in comparable ranges, appear much better defined in the case of the tetrahydrate.

In the case of $La_2(CO_3)_3.4H_2O$ two overtone bands, probably originated in components of ν_3, lying closely to the broad ν(OH) band, could be identified. On the other hand, the weak 2467

cm^{-1} IR band observed in the precursor, may be a combination between components of ν_1 and ν_3 (cf. also [24]).

The last band observed in both IR spectra (480 and 517 cm^{-1}, respectively) is probably related to La-O stretchings.

All the commented similarities in the spectroscopic behavior of the precursor and the tetrahydrate, suggest the presence of comparable La(III)/carbonate interactions in both compounds.

Acknowledgements. This work has been supported by CONICET and UNLP. The author is a member of the Research Career from CONICET.

REFERENCES

1. Wang, K., L. R. Li, Y. Cheng & B. Zhu (1999) *Coord. Chem. Rev.* **190/92**: 297-308.
2. Wang, K., Y. Cheng, X. Yang & R. Li (2003) *"Metal Ions in Biological Systems"* (A. Sigel & H. Sigel, Eds.), Marcel Dekker, New York, Vol. 40, pp. 707-51.
3. Jakupec, M.A., P. Unfried & B.K. Keppler (2005) *Rev. Physiol. Biochem. Pharmacol.* **153**: 101-11.
4. Fricker, S.P. (2006) *Chem. Soc. Rev.* **35**: 524-33.
5. Barta, C.A., K. Sachs-Barrable, J. Jia, K.H. Thompson, K.M. Wasan & C. Orvig (2007) *Dalton Trans.* **2007**: 5019-30.
6. Baran, E.J. (2007) *Lat. Amer. J. Pharm.* **26**: 626-34.
7. Caravan, P., J.J. Ellison, T.J. McMurry & R.B. Laufer (1999) *Chem. Rev.* **99**: 2293-352.
8. Roat-Malone, R.M. (2002) *"Bioinorganic Chemistry",* J. Wiley, Hoboken NJ.
9. Baran, E.J. (1995) *"Química Bioinorgánica",* McGraw-Hill Interamericana de España S.A., Madrid.
10. Fraústo da Silva, J.J.R. & R.J.P. Williams (1991) *"The Biological Chemistry of the Elements",* Clarendon Press, Oxford.
11. Edwards, R.M. (2002) *Curr. Opinion Pharmacol.* **2**: 171-6.
12. Loghman-Adham, M. (1999) *Pediatr. Nephrol.* **13**: 701-8.
13. Wallot, M., K.E. Bonzel, A. Winter, B. Geörger, B. Lettgen, M. Bald (1996) *Pediatr. Nephrol.* **10**: 625-30.
14. Joy, M.S., W.F. Finn (2003) *Am. J. Kidney. Dis.* **42**: 96-107.
15. Nagashima, K., H. Wakita, A. Mochizuki (1973) *Bull. Chem. Soc. Jpn.* **46**: 152-6.
16. Salutsky, M.L., L.L. Quill (1950) *J. Am. Chem. Soc.* **72**: 3306-7.
17. Wickleder, M.S. (2002) *Chem. Rev.* **102**: 2011-87.
18. Shinn, D.B., H.A. Eick (1968) *Inorg. Chem.* **7**: 1340-45.
19. Dal Negro, A., G. Rossi, V. Tazzoli (1977) *Amer. Mineral.* **62**: 142-6.
20. Turcotte, R.P., J.G. Sawyer, L. Eyring (1969) *Inorg. Chem.* **8**: 238-44.
21. Shirsat, A.N., M. Ali, K.N.G. Kaimal, S.R. Bharadwaj, D. Das (2003) *Thermochim. Acta* **399**: 167-70.
22. Paama, L., I. Pitkänen, H. Halttunen, P. Perämäki (2003) *Thermochim. Acta* **403**: 197-206.
23. Werner, P.E. (1969) *Ark. Kemi* **31**: 513-17.
24. Goldsmith, J.A., S.D. Ross (1967) *Spectrochim. Acta* **23A**: 1909-15.
25. Caro, P.E., J.O. Sawyer, L.R. Eyring (1972) *Spectrochim. Acta* **28A**: 1167- 73.
26. Ross, S.D. (1972) *Inorganic Infrared and Raman Spectra,* McGraw Hill, London.
27. Siebert, H. (1966) *Anwendungen der Schwingungsspektroskopie in der Anorganischen Chemie,* Springer, Berlin.
28. Nakamoto, K. (2009) *Infrared and Raman Spectra of Inorganic and Coordination Compounds,* 6th Edit., Part B, Wiley, New York.